A Simplified Scheme to Simulate Asymmetries Due to the Beta Effect in Barotropic Vortices

REBECCA J. ROSS AND YOSHIO KURIHARA

Geophysical Fluid Dynamics Laboratory/NOAA, Princeton University, Princeton, New Jersey

(Manuscript received 25 September 1991, in final form 27 November 1991)

ABSTRACT

A simplified scheme to generate vortex asymmetries due to the beta effect from an initially symmetric vortex on a beta plane is described. This approach, based on the time integration of the nondivergent barotropic vorticity equation, was developed to generate asymmetric vortex structure for inclusion in the initial conditions for the GFDL Hurricane Model. The simplification is derived from truncation of an azimuthal wavenumber expansion of the vorticity field variables. In order to determine the optimum lowest-order system, the influence of other wavenumbers (specifically 0, 2, and 3) on the asymmetric dipolar (wavenumber 1) structure and the associated vortex drift was investigated by comparing the results of a hierarchy of models differing in truncation level. The model truncated at wavenumber 2 and, including time-dependent symmetric flow, was chosen as the optimum system. Vortex drift tracks computed with this model compare very well with existing numerical model simulations. The models with a time-dependent symmetric flow produced systematically more westward- (less northward-) directed drift with slower speeds for cyclonic vortices than the models with time-independent symmetric flow. The results presented here clearly show the importance of including time-dependent symmetric flow in a simplified barotropic system. Discussion is developed regarding the interactions between the dipolar vortex and the wavenumber 0 and 2 flows. It appears acceptable to truncate the wavenumber expansion at wavenumber 2. The differences between the models with different levels of simplification increase when a larger initial vortex is used.

The generation of the asymmetric flow for incorporation into the hurricane model initial conditions involves several aspects of uncertainty not present in idealized cases. A particular problem is the development of overly strong far-field vorticity (i.e., lying much beyond the hurricane region) possibly resulting from inaccuracies in the symmetric wind profile. During the generation of asymmetries, this is suppressed by damping at large radii. Further investigation is needed into the sensitivity of the resulting hurricane drift to the symmetric wind profile and to the integration cutoff time.

1. Introduction

A simplified yet accurate scheme to generate the asymmetric vorticity structure that develops from integration of the barotropic vorticity equation on a beta plane is presented. This scheme represents one segment of a new initialization package designed to improve the representation of the tropical cyclone in the initial conditions for the Geophysical Fluid Dynamics Laboratory (GFDL) Hurricane Model. The inclusion of asymmetric structure in the initial vortex was motivated by the results of previous studies showing the important role that asymmetric structure can play in vortex propagation (for a review, see Smith et al. 1990). Earlier studies (e.g., Kasahara and Platzman 1963) had indicated that an initially stationary, symmetric vortex would develop a northwestward drift initiated by interaction with the earth's vorticity (the beta effect). Recent numerical simulations such as those by Chan and Williams (1987) or Smith et al. (1990) have focused on the detailed evolution of the asymmetric vorticity component and the resultant vortex propagation. One feature of these numerical simulations using the barotropic vorticity equation on a beta plane is the development of a quasi-steady vortex drift as the linear beta forcing reaches a semibalanced state with the nonlinear advection of the evolving vorticity field. Typically, the quasi-steady drift develops within one or two days and has a magnitude of 2–5 m s^{-1}. The exact magnitude and direction of the vortex propagation, however, is quite sensitive to the outer structure of the initial symmetric vortex, as was shown by Fiorino and Elsberry (1989, hereafter FE). Specifically, a larger vortex (i.e., one with stronger winds at outer radii) will develop a faster drift speed and a more westward direction. There are also some indications of a beta-induced drift in observational composite studies (i.e., George and Gray 1976). When estimates of the large-scale deep-layer mean environmental flow exclude the flow near the hurricane center—through filtering or exclusion of a region centered on the storm—the difference between this environmental "steering flow" and

Corresponding author address: Rebecca Ross, NOAA/ERL/GFDL, Princeton University, P.O. Box 308, Princeton, NJ 08542.

the observed track can be defined as the vortex propagation. Carr and Elsberry (1990) have reexamined a number of the composite studies in an attempt to determine how consistently the direction and speed of the vortex propagation agreed with the findings of numerical simulations such as those previously mentioned. They conclude that there is some evidence of consistency although data ambiguities prevent a definitive conclusion.

If the drift of a barotropic vortex on the beta plane is determined by the velocity at the vortex center, it is then solely defined by the dipolar (azimuthal wavenumber 1) vorticity component. Along this line, Smith and Ulrich (1990, hereafter SU) proposed a simple time-dependent analytical solution to the barotropic vortex drift problem. Although their scheme, based on a simplification of the vorticity equation, was fairly successful in simulating the vortex track for the first 12–24 h, the level of performance beyond that time was strongly dependent on the initial symmetric wind profile. In developing their solution method, SU limited their consideration to the azimuthal wavenumber 1 component and assumed a time-invariant symmetric profile. Peng and Williams (1990) have also simplified the barotropic vorticity equation by neglecting the possible small changes in the symmetric flow. However, the evolution of the wavenumber 1 vorticity depends on all wavenumber components. Recently, a further study by Smith (1991) using a higher-order correction to the zeroth-order solution showed improved results due to wavenumber 2 and 3 effects. In the present study, the influence of wavenumbers 0, 2, and 3 on the evolution of the wavenumber 1 vorticity and the associated vortex drift is investigated in a nonlinear prognostic framework. The goal of this investigation is to determine the lowest-order system that represents the vortex drift sufficiently accurately in comparison with full numerical models. While the scheme described here for determining the asymmetric flow is more computationally intensive than the SU scheme, it yields consistently accurate simulations of the vortex drift as compared with existing more complete numerical model simulations for periods extending to 72 h.

Currently, the density of observations and the horizontal resolution of operational (large-scale) analyses are inadequate to resolve a tropical cyclone structure including the asymmetry (e.g., Reeder et al. 1991). The introduction of a more realistic vortex structure or "bogus vortex" at the position of the storm offers a means of improving the initial condition of hurricane models. A number of authors have suggested the inclusion of asymmetric structure in the specification of a bogus vortex due to its importance in determining the vortex propagation (i.e., Peng and Williams 1990; SU). The long time scale—1 to 2 days—needed for development of the quasi-steady drift from an initially symmetric wind profile is a practical reason for inclusion of a pregenerated asymmetry in the initial conditions of a hurricane model. The resulting vortex propagation of a few meters per second can be a significant fraction of the total vortex movement, especially in a weak environmental flow. Even small displacements due to vortex propagation can lead to large differences in the vortex track at later times. The simplified method of generating asymmetric vorticity presented here has been successfully used in the bogus vortex initialization of the GFDL hurricane model.

In section 2, the barotropic vorticity equation is transformed into a form suitable for simplification. In section 3, the performance and behavior of simplified systems are analyzed to determine the optimum system. The subject of section 4 is the application of the derived optimum system to the specification of a bogus vortex. Problems requiring further attention are also discussed. Results from the present work are summarized in section 5.

2. Model formulation: Azimuthal wavenumber expansion of the vorticity equation

Beginning with the time-dependent nondivergent barotropic vorticity equation on a beta plane, the velocity and vorticity fields are decomposed into azimuthally symmetric and asymmetric parts

$$V = V_0 + V',$$
$$\zeta = \zeta_0 + \zeta', \tag{2.1}$$

where V is the velocity in the inertial frame. The vorticity equation in a reference frame that moves with the vortex drift velocity, C, becomes

$$\frac{\partial}{\partial t_m}(\zeta_0 + \zeta' + f) = -(V_0 + V' - C)\cdot\nabla(\zeta_0 + \zeta' + f), \tag{2.2}$$

where

$$\frac{\partial}{\partial t_m} = \frac{\partial}{\partial t_i} + C\cdot\nabla, \tag{2.3}$$

and the subscripts m and i indicate the moving and inertial frames. Separating (2.2) into symmetric and asymmetric parts gives

$$\frac{\partial \zeta_0}{\partial t_m} = -[(V' - C)\cdot\nabla\zeta']_0 - (V'\cdot\nabla f)_0,$$

$$\frac{\partial}{\partial t_m}\zeta' = -V_0\cdot\nabla\zeta' - (V' - C)\cdot\nabla\zeta_0 - [(V' - C)\cdot\nabla\zeta']' - (V\cdot\nabla f)', \tag{2.4}$$

where the nonlinear term $-(V' - C)\cdot\nabla\zeta'$ produces a symmetric contribution, $(-(V' - C)\cdot\nabla\zeta')_0$, as well as an asymmetric contribution, $(-(V' - C)\cdot\nabla\zeta')'$.

The term $-(V' \cdot \nabla f)$ also makes both a symmetric and an asymmetric contribution.

The simplification of (2.4) is derived from an azimuthal wavenumber expansion and truncation in a polar coordinate system. In this section, the wavenumber expansion of fields is achieved. Specifically, the vorticity is expanded into azimuthal wavenumber components (i.e., $\zeta = \zeta_0 + \zeta_1 + \zeta_2 + \zeta_3 + \cdots$ where suffixes indicate azimuthal wavenumber). The wind, **V**, is similarly expanded ($\mathbf{V} = V_0 + V_1 + V_2 + V_3 + \cdots$). In general, the amplitude and phase angle of each wavenumber component are functions of radius. To express this dependency, the vorticity field is discretized into "vortex rings" of width Δr. In each ring, a wavenumber component is represented by a constant amplitude and constant phase over that Δr. Thus, the wavenumber n vorticity in the ith vortex ring may be written as

$$\zeta_{n,i} = A_{n,i} \cos n(\theta - \varphi_{n,i}), \tag{2.5}$$

where $A_{n,i}$ and $\varphi_{n,i}$ denote the amplitude and phase in the vortex ring. The tendency equation for each $\zeta_{n,i}$, $n = 0, 1, 2, \cdots$ and $i = 1, 2, \cdots$, can then be obtained.

The velocity components are related to the vorticity by the general relationships between the streamfunction ψ, vorticity, and velocity (radial component v_r and tangential component v_t)

$$\nabla^2\psi = \zeta, \begin{cases} v_r = -\dfrac{1}{r}\dfrac{\partial\psi}{\partial\theta} \\ v_t = \dfrac{\partial\psi}{\partial r}. \end{cases} \tag{2.6}$$

As shown by Adem (1956) and utilized by SU, the solution of the Poisson equation for a vorticity distribution

$$\zeta(r, \theta) = F_n(r)\begin{bmatrix}\cos(n\theta)\\ \sin(n\theta)\end{bmatrix}$$

is

$$\psi(r, \theta) = \left[\frac{r^n}{2n}\int_0^r \rho^{-n+1}F_n(\rho)d\rho - \frac{r^{-n}}{2n}\int_0^r \rho^{n+1}F_n(\rho)d\rho + B_n(r)\right] \times \begin{bmatrix}\cos(n\theta)\\ \sin(n\theta)\end{bmatrix}, \tag{2.7}$$

where the condition that v_r and v_t vanish as $r \to \infty$ is satisfied if

$$\int_0^\infty \rho^{n+1}F_n(\rho)d\rho \quad \text{is finite and}$$

$$B_n(r) = \left(-\frac{r^n}{2n}\right)\int_0^\infty \rho^{-n+1}F_n(\rho)d\rho. \tag{2.8}$$

Using (2.8) and (2.7) in (2.6), the following formulas determining the radial and tangential velocity components of wavenumber n for a given distribution of $F_n(r)$ are obtained:

$$v_{n,r}(r, \theta) = \frac{1}{n}[p_n(r) + q_n(r)]\begin{bmatrix}\sin(n\theta)\\ -\cos(n\theta)\end{bmatrix},$$

$$v_{n,t}(r, \theta) = [p_n(r) - q_n(r)]\begin{bmatrix}\cos(n\theta)\\ \sin(n\theta)\end{bmatrix}, \tag{2.9}$$

where

$$p_n(r) = -\frac{r^{n-1}}{2}\int_r^\infty \rho^{-n+1}F_n(\rho)d\rho,$$

$$q_n(r) = -\frac{r^{-n-1}}{2}\int_0^r \rho^{n+1}F_n(\rho)d\rho. \tag{2.10}$$

If the vorticity field is rotated by φ, as in (2.5), the angle factors of the velocity components in (2.9) become $n(\theta - \varphi)$ instead of $n\theta$. By analytically predetermining the incremental contributions of each vortex ring (over which F_n is constant) to p_n and q_n for its own and other vortex rings, the evaluation of the velocity components of wavenumber n in a ring becomes simply a weighted summation of the wavenumber n vorticity over all vortex rings. In particular, the vortex drift, C, when assumed to be equal to the velocity at the center, depends only on ζ_1. From (2.5), the eastward and northward components of the vortex drift are

$$C_E = -\frac{\Delta r}{2}\sum_i A_{1,i}\sin(-\varphi_{1,i}),$$

$$C_N = -\frac{\Delta r}{2}\sum_i A_{1,i}\cos\varphi_{1,i}. \tag{2.11}$$

To derive the tendency equation for ζ_n; $n = 0, 1, 2, \cdots$, the vector products on the right-hand side of (2.4) have to be grouped by resultant wavenumber. The interaction between the two fields of wavenumber n and m in the advection terms, that is, $(-V_n \cdot \nabla\zeta_m)$ or $(-V_m \cdot \nabla\zeta_n)$, will produce forcing for the ζ_{n+m} and ζ_{n-m} components. In particular, the term $(-V_n \cdot \nabla\zeta_n)_0$ projects onto the ζ_0 tendency equation. The term $C \cdot \nabla\zeta_n$ and the beta term, $-V_n \cdot \nabla f$, contribute to the ζ_{n+1} and ζ_{n-1} tendencies, because the constant fields C and ∇f are wavenumber 1 fields in the azimuthal wavenumber domain. The vorticity equation projected onto wavenumber components will be simplified in the next section by the wavenumber truncation.

3. Simplified models

The goal of this work is to determine the highest degree of azimuthal wavenumber truncation that can adequately describe the vortex drift of existing full numerical model simulations. The vortex drift itself de-

pends on the evolution of dipolar vorticity (wavenumber 1 component).

a. *Performance of truncated models*

The model design has allowed easy testing of the importance of other wavenumbers in accurately generating the wavenumber 1 vorticity field. The hierarchy of models listed in Table 1 were devised by varying the level of truncation and by including or excluding the time dependency of the symmetric (wavenumber 0) flow. Of course, the form of the vorticity tendency equation for each wavenumber component is affected by the level of truncation. For example, each additional wavenumber will result in additional advection terms in the wavenumber 1 tendency equation. Also, given that the wind of the nth wavenumber component affects the wavenumber $n-1$ and $n+1$ tendency equations through the beta term, changes in truncation can modify the beta forcing of the wavenumber tendency equations. The simplest of these models is model $K1$, which is truncated at wavenumber 1 and uses a fixed symmetric field throughout the integration. The analytic solution (including correction) proposed by SU is similar to model $K1$. Model $K01$ is also truncated at wavenumber 1 but includes a time-dependent symmetric flow. Similarly, models $K12$ and $K012$ are both truncated at wavenumber 2 and differ in the treatment of the symmetric flow; model $K12$ uses a fixed symmetric flow while model $K012$ includes a time-dependent symmetric flow. Finally, model $K0123$ is truncated at wavenumber 3 and also includes a time-dependent symmetric flow.

The initial condition for the time integration of the simplified model specifies the tangential wind profile of an initially symmetric vortex. In this study, the time integration proceeds using a time step of 60 s and a centered time differencing after an initial forward step. In the results of section 3 the chosen domain size and radial resolution were determined to be appropriate by verifying the stability of the results with a larger domain and finer resolution. For example, a domain of radius 3600 km was sufficient for most of the vortex profiles, but for the largest vortex profile used, it was necessary to use a domain radius of nearly 7000 km to adequately capture the development of the far-field vorticity. For most profiles $\Delta r = 30$ km was sufficient but for the smallest vortex profile it was necessary to use $\Delta r = 20$ km.

TABLE 1. Summary of the model variations.

Model	Symmetric flow	Truncation level (wavenumber)
$K1$	fixed	1
$K01$	time dependent	1
$K12$	fixed	2
$K012$	time dependent	2
$K0123$	time dependent	3

The five models are first compared with each other using the "standard" symmetric profile of SU. That profile (see their Fig. 1a) has a maximum velocity of 40 m s^{-1} at a radius of 100 km and decreases to 15 m s^{-1} at a radius of 300 km. The differences between the model results can be seen in Fig. 1, which shows the evolution of the vortex drift speed and direction. The quasi-steady drift that develops in the full numerical model simulations after 36–48 h is not reproduced by the simplest model ($K1$). In fact, the $K1$ drift speed in Fig. 1a is continually increasing with time. The most complete models ($K012$ and $K0123$) do stabilize at a relatively steady drift speed of $\sim$2.8 m s^{-1} after about 48 h. The inclusion of the time-dependent symmetric flow is very important for the development of a quasi-steady drift speed (compare $K1$ with $K01$). It also shifts the drift direction more westward (Fig. 1b). Interestingly, the addition of wavenumber 2 appears to influence the drift evolution in a manner similar to the symmetric flow feedback. For example, the model $K12$ drift speed initially follows that of model $K1$ (while the amplitude of wavenumber 2 is still small) but gradually stabilizes at a value of $\sim$3.7 m s^{-1}, or 0.9 m s^{-1} faster than in models $K012$ and $K0123$. Similarly, the drift speed of model $K012$ initially follows that of $K01$, but as the influence of wavenumber 2 increases the speed of model $K012$ stabilizes, while that of model $K01$ continues to slowly increase. The drift directions in $K12$ and $K012$ are, respectively, more westward than in $K1$ and $K01$. For the five model types the drift speed seems fairly steady while the drift direction is more variable (Fig. 1b). This is also apparent in the numerical results in DeMaria (1985, Fig. 2). In general, including the wavenumber 2 component and a time-dependent symmetric flow each appears to decrease the vortex drift speed. The feedback to the symmetric flow is more important early in the integration when the wavenumber 2 amplitude is still small. Finally, the close agreement between the results of models $K012$ and $K0123$ for both the drift speed and direction suggests that it is permissible to truncate at wavenumber 2.

These conclusions regarding drift speed and direction for the standard vortex of SU also hold for other vortex profiles (Table 2), including the small vortex of SU, the DeMaria profile, and the FE basic and weak–large profiles. The size and shape of these profiles are indicated in Table 2 by the maximum wind, V_{max}, the radius of maximum wind, R_{max}, and a size indicator (the radius where the velocity drops to 5 m s^{-1}). Also in Table 2 are the 48-h differences in track position between models $K1$ and $K012$ representing the spread among the five models. As the size of the initial vortex increases, the differences between the models also increase, which suggests the importance of including both the time dependency of the symmetric flow and the wavenumber 2 component as the vortex size becomes

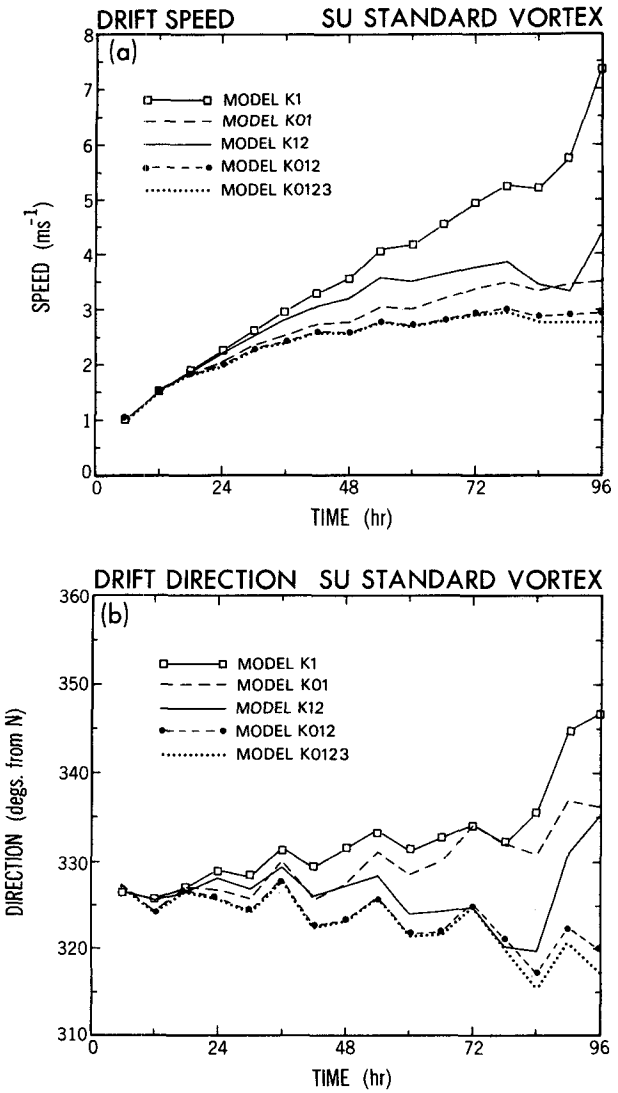

FIG. 1. Evolution of (a) vortex drift speed (m s^{-1}) and (b) vortex drift direction (deg, clockwise from north) for the five model variations, plotted at 6-h intervals from 96-h integrations, using the SU standard vortex as input.

larger. The 72-h vortex drift tracks for models *K*1 and *K*012, using the SU "standard" and "small" profiles, are shown in Fig. 2 and indicate that the track differences in Table 2 are due to systematically larger drift speeds and more northward drift directions when the symmetric component is held fixed and when truncation occurs at wavenumber 1. This is true for all the profiles considered.

b. Interaction of wavenumber 1 asymmetry with other components

As indicated from (2.4), the structure of the dipolar vorticity (wavenumber 1 component) and, hence, the vortex drift is influenced by the feedback process between the dipole and the symmetric component, as well as by the nonlinear interaction among different wavenumber components. In particular, the wavenumber 0 field influences the wavenumber 1 tendency through the interaction of wavenumbers 0 and 1 in the advection terms $-V_0 \cdot \nabla\zeta_1$ and $-V_1 \cdot \nabla\zeta_0$ and also through the beta forcing term $-V_0 \cdot \nabla f$. Accordingly, when a model includes a time-dependent symmetric field, the wavenumber 1 tendency will be affected by the modification of the symmetric flow. Changes in the symmetric flow lead to a general decrease in the tangential wind and the development of weak anticyclonic flow at outer radii (see FE, Fig. 6). The magnitude of these changes varies with radius and also depends on the initial symmetric profile. The largest change in the SU standard profile at 48 h was 0.75 m s^{-1} at a radius of 900 km, while that of the FE weak–large profile was 3.05 m s^{-1} at a radius of 1100 km. The radial profile of the change in the symmetric flow for the SU standard vortex at 24 h is quite similar to recent results by Smith (1991, Fig. 4). The wavenumber 2 component also modifies the wavenumber 1 tendency through nonlinear advection and beta forcing. Note that the wavenumber 0 and 2 forcing to the wavenumber 1 field then directly affects the wavenumber 0 and 2 tendencies via advection $-V_1 \cdot \nabla\zeta_1$ and wavenumber 1 beta forcing $-V_1 \cdot \nabla f$. By considering the differences in these feedback processes among the models it is possible to qualitatively explain the differences in vortex drift that were presented in section 3a.

The ζ_1 field that is induced by the initial symmetric flow, V_0, through the beta forcing term, $-V_0 \cdot \nabla f$, may be expressed at an early time Δt as

$$\zeta_1 = \Delta t(-\beta V_0)\cos(\theta - \varphi). \qquad (3.1)$$

TABLE 2. Summary of the input vortex profiles and comparisons of 48-h position differences. SU: Smith and Ulrich (1990), FE: Fiorino and Elsberry (1989), DeMaria: De Maria (1985).

Vortex profile	V_{max} (m s^{-1})	R_{max} (km)	Size radius (km) where V = 5 m s^{-1}	Difference (km) in 48-h positions of *K*1 and *K*012	Difference (km) between 48-h positions of *K*012 and numerical simulation
SU small	40	100	300	25	10
SU standard	40	100	480	56	24
DeMaria	30	80	670	72	24
FE basic	35	100	475	48	4
FE weak–large	20	100	950	460	91

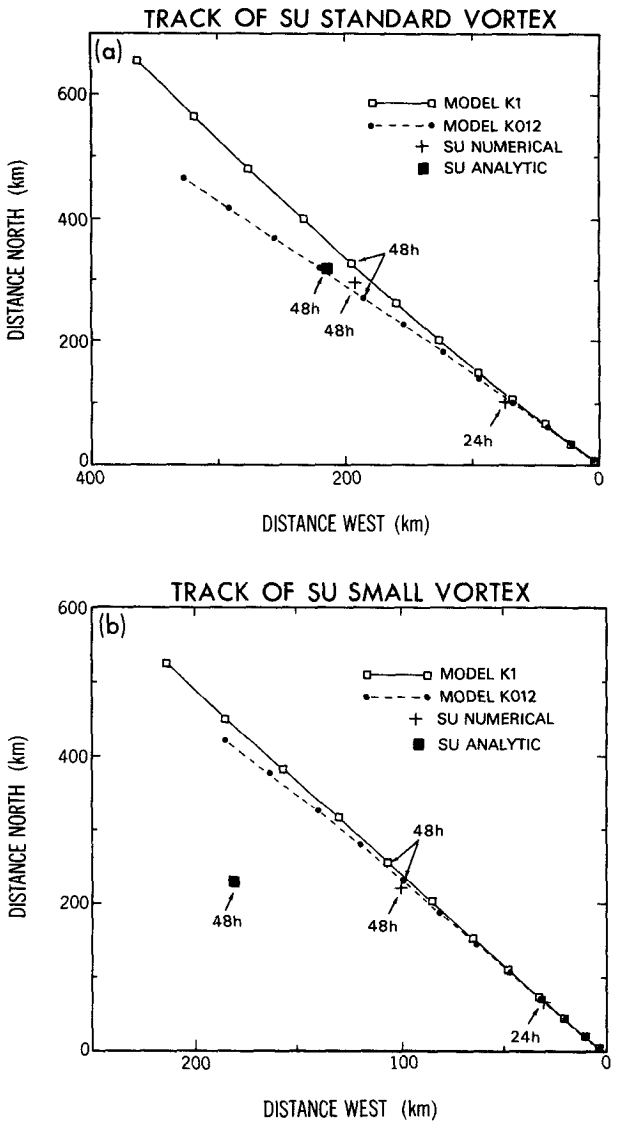

FIG. 2. Vortex tracks of models $K1$ and $K012$ for 72 h of integration plotted using (a) the standard vortex and (b) the small vortex of SU. Vortex positions are indicated at 6-h intervals. Also shown are the corresponding 24-h and 48-h positions of the Smith et al. (1990) numerical model results as well as the 48-h positions of the SU analytic solution.

For the purpose of this qualitative argument, radial variation of φ is ignored and it is assumed that $0 < \varphi < \pi/2$. From (2.9) and (2.10) the corresponding radial and tangential components of V_1 are obtained as

$$v_{1,r} = \Delta t(p_1 + q_1)\sin(\theta - \varphi),$$
$$v_{1,t} = \Delta t(p_1 - q_1)\cos(\theta - \varphi), \qquad (3.2)$$

where

$$p_1(r) = \frac{\beta}{2}\int_r^\infty V_0 d\rho, \quad q_1(r) = \frac{\beta}{2r^2}\int_0^r \rho^2 V_0 d\rho.$$

If V_0 vanishes for $r \geq R$, then ζ_1, as expressed by (3.1), is confined within R. The asymmetric flow, V_1, is also radially confined (i.e., $V_1(r) = 0$ for $r \geq R$) if the total relative angular momentum of the vortex is zero; that is, if $q_1(R) = 0$ (an isolated vortex). In the case of a cyclonic vortex (in the Northern Hemisphere, $V_0(r) > 0$ for $r < R$) where $q_1(R) > 0$, the asymmetric flow, V_1, is produced at $r = R$ and beyond. In either case, the vortex drift becomes

$$C_E = -\Delta t p_1(0)\sin\varphi,$$
$$C_N = \Delta t p_1(0)\cos\varphi. \qquad (3.3)$$

The drift is west of due north provided that $p_1(0) > 0$. This is an estimate of the drift velocity in model $K1$. The interaction effects between the dipolar vorticity and other vorticity components can now be estimated by considering the beta forcing due to the induced flow, $-V_1 \cdot \nabla f$. Because the meridional component of V_1 is

$$v_{1,r}\sin\theta + v_{1,t}\cos\theta = \Delta t[p_1\cos\varphi - q_1\cos(2\theta - \varphi)], \qquad (3.4)$$

the preceding forcing produces new vorticity $\Delta\zeta_0$ and ζ_2;

$$\Delta\zeta_0 = \Delta t(-V_1 \cdot \nabla f)_0 = -\Delta t^2\beta p_1\cos\varphi, \qquad (3.5)$$

$$\zeta_2 = \Delta t(-V_1 \cdot \nabla f)_2 = \Delta t^2\beta[q_1\cos(2\theta - \varphi)]. \qquad (3.6)$$

The flow corresponding to $\Delta\zeta_0$ is

$$\Delta V_0 = -\Delta t^2\beta\cos\varphi\,\frac{1}{r}\int_0^r \rho p_1(\rho)d\rho. \qquad (3.7)$$

Accordingly, for an initial cyclonic vortex, an anticyclonic flow ($\Delta V_0 < 0$) develops that reduces the initial flow, V_0. The ζ_1 tendency of model $K01$ (or model $K012$) can then be expressed as the modification of the model $K1$ tendency by the feedback due to ΔV_0

$$\left(\frac{\partial\zeta_1}{\partial t}\right)_{K01} = \left(\frac{\partial\zeta_1}{\partial t}\right)_{K1} - \Delta V_0\beta\cos\theta. \qquad (3.8)$$

When $V_0 > |\Delta V_0|$, the last term in (3.8) effectively decreases the beta forcing of model $K1$. Thus, $(\zeta_1)_{K01}$ is weaker than $(\zeta_1)_{K1}$ except in regions where $V_0 < |\Delta V|$. In Fig. 3 the wavenumber 1 vorticity field of model $K01$ is compared with that of model $K1$ after 48 h of integration with the SU standard vortex. The two fields are qualitatively very similar but the $K01$ wavenumber 1 vorticity has a generally smaller amplitude than $K1$ over the region of the primary vorticity gyres. As discussed, this difference is directly related to the induced anticyclonic flow associated with model $K01$. Where the $K01$ symmetric flow becomes anticyclonic ($V_0 < |\Delta V_0|$), the time tendency of $(\zeta_1)_{K01}$ expressed by (3.8) is 180 degrees out of phase with that of $K1$. The presence of the secondary extrema in Fig. 3 (at a radius of ~600 km) with a phase angle of approximately 5 degrees in the model $K01$ ζ_1 field implies that equation (3.8) is a good approximation to the vorticity tendency at outer radii even at 48 h. Note that a

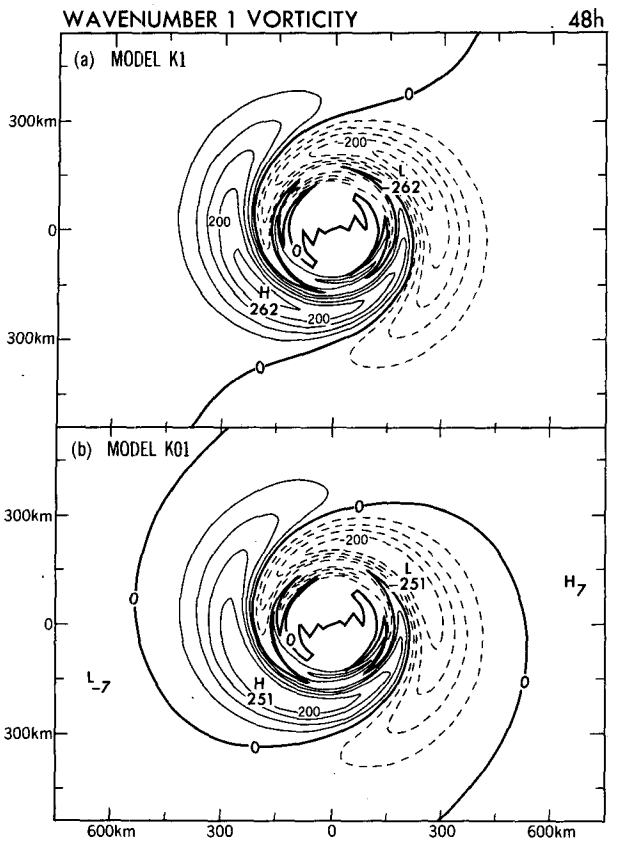

FIG. 3. Wavenumber 1 vorticity (s^{-1}) of (a) model $K1$ and (b) model $K01$ after 48 h of integration using the SU standard vortex as input. Contour interval is 50. $\times 10^{-7}$ s^{-1}. The region shown is approximately one-fifth of the total integration domain area.

change in the advection of asymmetric vorticity [omitted in (3.8)] with the development of anticyclonic flow at outer radii in model $K01$ would reinforce the ζ_1 tendency phase difference between models $K1$ and $K01$. From (3.8), the difference in the vortex drift between the models $K01$ and $K1$ becomes

$$\Delta C_E = 0,$$

$$\Delta C_N = \frac{(\Delta t)\beta}{2}\int_0^\infty \Delta V_0 dr. \qquad (3.9)$$

For a cyclonic vortex, ΔC_N is negative (because $\Delta V_0 < 0$). Comparison of (3.9) and (3.3) indicates that the drift of a cyclonic vortex in model $K01$ is slower and more westward (less northward) than in model $K1$. This agrees with the results in section 3a. In general, the change in drift direction due to ΔC_E and ΔC_N, measured counterclockwise from north, is from

$$\arctan\left(\frac{-C_E}{C_N}\right) \quad \text{to} \quad \arctan\left(\frac{-(C_E+\Delta C_E)}{(C_N+\Delta C_N)}\right). \qquad (3.10)$$

In section 3a, it was shown that the changes in the vortex drift when wavenumber 2 vorticity is included are similar to the drift changes due to the inclusion of a time-dependent symmetric flow. Specifically, the drift speed of model $K12$ was slower than that of model $K1$. By analogy with (3.8) and again assuming the primary contribution is through the beta forcing, the wavenumber 1 vorticity tendency of model $K12$ can be written as

$$\left(\frac{\partial \zeta_1}{\partial t}\right)_{K12} = \left(\frac{\partial \zeta_1}{\partial t}\right)_{K1} + (-V_2\cdot\nabla f)_1. \qquad (3.11)$$

The ζ_2 feedback to the ζ_1 tendency can be estimated by obtaining the V_2 field corresponding with ζ_2 of (3.6) and computing $(-V_2\cdot\nabla f)_1$. After some manipulation, one obtains

$$(-V_2\cdot\nabla f)_1 = \frac{\Delta t^2\beta}{8}\left\{3r\int_r^\infty \frac{1}{\mu} q_1(\mu)d\mu - \frac{1}{r^3}\int_0^r \mu^3 q_1(\mu)d\mu\right\}\cos(\theta-\varphi). \qquad (3.12)$$

For a cyclonic vortex (e.g., $V_0 \propto r^{-1}$ for $r < R$ and $V_0 = 0$ for $r \geq R$), the amplitude of the $\cos(\theta-\varphi)$ term in (3.12) is positive and ζ_1 in model $K12$ is thus weaker than in model $K1$. This conclusion also applies to the comparison of the ζ_1 tendencies of model $K012$ and model $K01$. Because the feedback to ζ_1 from ζ_2 [see (3.11)] is qualitatively similar to that from the ζ_0 change [see (3.8)], the amplitude of ζ_1 should be even weaker in model $K012$ than in $K01$ or $K1$. This is found to be the case. In particular, the magnitude of the ζ_1 maximum at 48 h decreases from 2.62×10^{-5} s^{-1} in model $K1$ to 2.51×10^{-5} in model $K01$ (see Fig. 3) and to 2.17×10^{-5} in model $K012$. The vortex drift speeds are similarly ordered.

In contrast, the wavenumber 3 fields affect the wavenumber 1 tendency only indirectly, by combining with wavenumber 2 in nonlinear advection. Wavenumber 3 flow does not contribute to wavenumber 1 beta forcing. The small difference between the drift velocities of models $K012$ and $K0123$ is consistent with the smaller degree of influence, which wavenumber 3 vorticity adds to the system as compared with wavenumbers 0 or 2.

Based on the model comparisons of section 3a and the reasoning of this section, model $K012$ is chosen as the optimum lowest-order system.

c. *Comparison of the optimum truncated model with nontruncated models*

Results from model $K012$ are compared with those from existing nontruncated numerical models for the different initial profiles listed in Table 2. Model $K012$ shows consistent agreement with the numerical results. For example, DeMaria (1985) found a quasi-steady drift speed of ~2.5 m s^{-1} and direction of 315–320 deg for a numerical model, while the $K012$ scheme using the same initial profile developed a speed of ~2.6 m s^{-1} and a heading of 313–319 deg. In Fig. 2, the 24-h and 48-h positions of the numerical model vortex simulation of Smith et al. (1990) (see Figs. 5 and 7 in

SU) are shown for comparison with the 72-h vortex drift tracks of model *K*012. Over the first 24 h the *K*012 track agrees very well with the numerical model result, and the agreement with the numerical results at 48 h is still quite good. The drift in this model is a little too fast compared with the 48-h numerical model position for the small vortex case, while it is a little slow for the standard vortex case.

The 48-h position of the SU analytic solutions (including correction) are denoted by the solid square. The SU solution works quite well for the standard vortex but is less successful at determining the track of the small vortex. Because the performance of model *K*1 represents a substantial improvement over the SU result with the small vortex profile, it seems that the SU correction scheme does not adequately simulate the vorticity advection for that case. The final column of Table 2 shows the difference in the 48-h track positions between the numerical models and model *K*012 for the SU profiles and for the FE basic and weak–large vortex profiles. The differences are quite small except for the weak–large vortex. A possible explanation for this larger difference of the weak–large vortex is that the numerical results of FE are affected by the relatively small domain used (4000 km compared with the 7000 km used here).

4. Application to the bogus vortex specification

Model *K*012 was used to generate the asymmetric component of the bogus vortex in the GFDL Hurricane Model initialization scheme. The details of the complete initialization scheme and the forecast improvement will be reported in separate papers. However, aspects of the implementation influencing the resultant asymmetric flow are worthy of discussion here.

The first issue is the determination of the integration cutoff time. In the present scheme, the vortex drift slowly becomes quasi-steady. This slowness justifies prescribing an asymmetric flow in a bogus vortex. On the other hand, it also implies that the symmetric wind profile should be relatively constant over the integration period—this is not necessarily true in actual cases. In fact, the actual asymmetry depends on the vortex history. The cutoff time may be used to adjust for the known past development of the hurricane. If the vortex is in the development stage it is possible that the asymmetry is weaker because the symmetric profile may have undergone a larger change (in the preceding 24 h) than in the corresponding case of a mature hurricane. To account for this, the integration period for an immature cyclone can be shortened, thus limiting the asymmetric development. However, this modification of the integration period is rather ad hoc and should be carefully tested before any conclusion is reached as to its usefulness.

Probably the most important aspect of the application to real hurricanes is the problem of accurately specifying the symmetric wind profile. In actual cases, the symmetric wind profile must be determined from fairly limited observations, particularly at outer storm radii. An additional complication (specific to this initialization scheme) arises from the procedure of partitioning the initial condition fields into an environmental component and a vortex component. Thus, there is a degree of unavoidable uncertainty in the symmetric profile and also in the asymmetric flow derived from it. The initial symmetric vortex is defined for each actual case over a cylindrical domain of appropriate radius, r_b, centered on the storm position. Tests with actual hurricanes suggest that the radius of the integration domain for the asymmetry generation, however, should usually be much larger than r_b. This is due to the development of far-field vorticity from a nonisolated vortex (i.e., a vortex with a nonzero total relative angular momentum). Then, the uncertainties in the symmetric profile at large radii may result in an erroneous far-field vorticity development. In tests with actual huge hurricane profiles, the development of asymmetric vorticity at outer radii with this scheme appears to be too strong. Shapiro and Ooyama (1990) have shown that relatively small changes in the initial symmetric profile at outer radii can significantly change the total relative angular momentum and thus affect the extent of far-field vorticity development.

One approach to limiting the far-field vorticity development might be to modify the initial symmetric profile such that the total relative angular momentum is zero. However, this was avoided in order to preserve the observational nature of the symmetric profile. Rather, the approach used in the initialization scheme is to incorporate damping in the vorticity equation that affects only the asymmetric wavenumber components at large radii. Using an implicit Newtonian damping form, the damped vorticity is obtained as

$$(\zeta_n)_{\text{damped}} = \frac{(\zeta_n)_{\text{predicted}}}{(1 + 2\Delta t/\tau)} \quad (n = 1, 2), \quad (4.1)$$

where $(\zeta_n)_{\text{predicted}}$ means the prediction by model *K*012, Δt is the time step, and τ is the damping time scale where for $r > r_{\text{damp}}$,

$$\frac{1}{\tau(r)} = \frac{1}{\tau_b}\left(\frac{r - r_{\text{damp}}}{r_b - r_{\text{damp}}}\right). \quad (4.2)$$

Because an error in the far-field vorticity does influence the velocity near the center, the damping must be done throughout the time integration. In (4.2), r_{damp} is the radius where damping begins and τ_b is the damping time constant valid at r_b. The damping is zero at radius r_{damp} and increases out to the edge of the integration domain. The effect of the damping on the vortex drift is to generally decrease the drift speed while the drift direction becomes more westward and less northward.

5. Remarks

A simplified scheme has been described to generate beta-effect asymmetries from an initially symmetric

vortex on a beta plane. The motivation for developing this scheme was to include asymmetric structure in a new initialization package designed to improve the representation of the tropical cyclone in the initial conditions for the GFDL Hurricane Model. The simplicity of this scheme, which is based on the time integration of the barotropic vorticity equation, results from the truncation of an azimuthal wavenumber expansion of the vorticity field. A particular goal of this study was to determine the lowest-order system that can adequately simulate the vortex drift. The basis for comparison of simulated vortex drift was the published results of numerical barotropic model studies examining asymmetric structure. Tests of the influence that other wavenumbers (specifically 0, 2, and 3) have on the structure of the wavenumber 1 vorticity controlling the vortex drift indicate that it is acceptable to truncate the wavenumber expansion at wavenumber 2. There is little difference in vortex drift track between the model truncated at wavenumber 3 and that truncated at wavenumber 2. The results presented here clearly indicate the importance of including a feedback modification of the symmetric vorticity in order to accurately simulate the time evolution of the dipolar vorticity field. Specifically, in the models using an invariant symmetric flow, a systematically too northward drift direction as well as excessively large drift speeds developed. The wavenumber 2 forcing of the wavenumber 1 vorticity tendency influences the vortex drift in much the same manner as the symmetric flow feedback; namely, it reduces the drift speed and produces a more westward angle. Because the wavenumber 2 component is initially zero, the symmetric flow feedback effect will be larger during earlier periods. However, the improvement in vortex drift simulation at extended periods produced by including wavenumber 2 shows the importance of this component. The differences between the five models with different degrees of simplification increase when larger initial vortices are used. Vortex drift tracks computed with the optimum scheme compare very well with existing, more complete numerical model simulations.

The generation of asymmetric flow for a bogus vortex specification in hurricane models involves several issues not present in the idealized cases examined here. In particular, the importance of an accurate specification of the initial symmetric flow profile and the determination of the integration cutoff time are two aspects of this scheme that need to be considered. In addition, damping of the asymmetric vorticity at large radii was used to control the development of far-field vorticity lying beyond the region of bogus vortex specification. There are indications that the far-field vorticity that develops in this model (without damping) is too strong when a very large initial vortex is used. This may be related to inaccuracies in the symmetric profile. The sensitivity to the damping parameters should be examined more carefully. Finally, for observed vortices embedded in an environmental flow, additional factors influence the vortex propagation. For instance, besides the beta effect, vorticity gradients of the environmental field were shown by DeMaria (1985) to affect the vortex propagation. Environmental vorticity gradients are more difficult to incorporate in a simplified scheme because of spatial and temporal variations. Smith (1991) recently showed the effects of horizontal shear on vortex propagation and structure change. Factors such as the vertical wind shear may also influence the vortex drift. The significance of environmental flow features (in the initial data) for the bogus vortex drift should be more thoroughly investigated.

Acknowledgments. The authors would like to thank Gareth P. Williams and Robert E. Tuleya for their valuable comments on the original version of this manuscript. Also, they appreciate the stimulating discussion with Roger K. Smith on this topic. Finally, thanks and credit are given to Phil Tunison, Cathy Raphael, and Jeff Varanyak for preparing the figures.

REFERENCES

Adem, J., 1956: A series solution for the barotropic vorticity equation and its application in the study of atmospheric vortices. *Tellus,* **8,** 364–372.

Carr, L. E., and R. L. Elsberry, 1990: Observational evidence for predictions of tropical cyclone propagation relative to environmental steering. *J. Atmos. Sci.,* **47,** 542–546.

Chan, J. C., and R. T. Williams, 1987: Analytical and numerical studies of the beta-effect in tropical cyclone motion. Part I: Zero mean flow. *J. Atmos. Sci.,* **44,** 1257–1265.

DeMaria, M., 1985: Tropical cyclone motion in a nondivergent barotropic model. *Mon. Wea. Rev.,* **113,** 1199–1210.

Fiorino, M., and R. L. Elsberry, 1989: Some aspects of vortex structure related to tropical cyclone motion. *J. Atmos. Sci.,* **46,** 975–990.

George, J. E., and W. M. Gray, 1976: Tropical cyclone motion and surrounding parameter relationships. *J. Appl. Meteor.,* **15,** 1252–1264.

Kasahara, A., and G. W. Platzman, 1963: Interaction of a hurricane with the steering flow and its effect upon the hurricane trajectory. *Tellus,* **15,** 321–335.

Peng, M. S., and R. T. Williams, 1990: Dynamics of vortex asymmetries and their influence on vortex motion on a β plane. *J. Atmos. Sci.,* **47,** 1987–2003.

Reeder, M. J., R. K. Smith, and S. Lord, 1991: The detection of flow asymmetries in the tropical cyclone environment. *Mon. Wea. Rev.,* **119,** 848–854.

Shapiro, L. J., and K. V. Ooyama, 1990: Barotropic vortex evolution on a beta plane. *J. Atmos. Sci.,* **47,** 170–187.

Smith, R. K., 1991: An analytic theory of tropical-cyclone motion in a barotropic shear flow. *Quart. J. Roy. Meteor. Soc.,* **117,** 685–714.

——, and W. Ulrich, 1990: An analytical theory of tropical cyclone motion using a barotropic model. *J. Atmos. Sci.,* **47,** 1973–1986.

——, ——, and G. Dietachmayer, 1990: A numerical study of tropical cyclone motion using a barotropic model. Part 1. The role of vortex asymmetries. *Quart. J. Roy. Meteor. Soc.,* **116,** 337–362.